Results: The distribution of carcinomas by molecular classification and OncDX recurrence score groups is listed in Table 1. For the 26 Luminal-A carcinomas, the mean/ median OncotypeDX recurrence scores were 13.4/ 13.5 respectively (range, 8 – 20). None of the Her2-V, Her2-C, or basal molecular groups had low recurrence risk OncotypeDX scores. Of the 40 high OncotypeDX recurrence score cases, 0 were luminal-A, 9 (22.5%) were Luminal-B, 8 (20.0%) were Her2-V, 14 (35.0%) were Her2-C, and 9 (22.5%) were basal phenotype. All of the Her2-C and basal phenotype cases had very-low level positive ER values.

Conclusions: The Sorlie-based IHC molecular classification groups and OncotypeDX recurrence score overlapped to a substantial degree. Luminal A group carcinomas were highly correlated with low OncDX recurrence score. Although ER+, the high recurrence risk OncDX score group was comprised of a mixture of neoplasms including Her2-classic and basal phenotype neoplasms.

OncotypeDX Recur. Score vs Molec. Class. Group

	OncDX Recurrence Score			
Molec. Class. Group	**Low**	**Intermediate**	**High**	**Total Cases**
Luminal-A	24 (92.3%)	2 (7.7%)	0	26 (100%)
Luminal-B	5 (7.4%)	53 (79.1%)	9 (13.4%)	67 (100%)
Her-Variant	0	7 (46.7%)	8 (53.3%)	15 (100%)
Her2-Classic	0	2 (12.5%)	14 (87.5%)	16 (100%)
Basal	0	2 (18.1%)	9 (81.8%)	11 (100%)

234 Correlations of Chromosome 17 Number with Her2/neu Gene Copy Number by FISH and Protein Expression by IHC in Breast Invasive Ductal Carcinoma

S Zhang, SS Shah. SUNY-Upstate Medical University, Syracuse, NY.

Background: Her2/neu gene amplification by fluorescent in-situ hybridization (FISH) and protein expression by immunohistochemistry (IHC) have been used for prognosis and guiding treatment of invasive ductal carcinoma of the breast with Trastuzumab. FISH assay is considered as a gold standard in the interpretation of cases with equivocal IHC results. Polysomy of chromosome 17, at which Her2/neu is located, can be identified in 20-30% of cases tested and it is unclear whether this affects the interpretation of FISH and IHC results. The aim of this study was to correlate the chromosome 17 number with Her2/neu gene copies by FISH and protein expression by IHC.

Design: A retrospective analysis of invasive ductal carcinomas diagnosed over 18 months revealed 90 cases that were evaluated for Her2/neu gene by FISH and protein expression with IHC. Clinical history, histologic slides and FISH results were evaluated. The Her2/neu/CEP17 ratio, Her2/neu copy number per nucleus and number of chromosome 17 per nucleus was calculated. The FISH data were compared with IHC results through computing correlation coefficients (CC) and statistical analysis.

Results: FISH for Her2/neu gene was performed on 90 women (Mean age 57.9 years; Range 26-92 years). The average chromosome 17 number per nuclei was 2.4 (1.5 to 3.95). There were strong associations of IHC grading with FISH Her2/neu/cep 17 ratio (CC 0.51, $p < 0.001$) and Her2/neu signal/nucleus (CC 0.51, $p < 0.001$), as expected. In addition, we found significant correlation between number of chromosome 17/nucleus and Her2/neu signal per nucleus (CC 0.44, $p < 0.001$). However, no correlation was seen between number of chromosome 17/nuclei and either IHC grading (CC 0.18, $p > 0.05$) or Her2/neu/cep17 ratio (CC 0.17, $p > 0.05$). Polysomies (≥2.7 chromosome /nuclei) were identified in 23 of 90 (25.6%) cases.

Conclusions: Polysomy occurs commonly in invasive ductal breast carcinomas. Although the chromosome 17 copy number influences the total Her2/neu signal per nucleus, it affects neither the ratio of Her2/neu/cep17 by FISH nor the protein expression by IHC.

235 Triple Approach to Core Needle Biopsy (CNBX) of Breast Masses with and without Image-Guidance: Follow-Up Analysis of 673 Patients with Benign CNBX Diagnoses

Z Zhang, M Raoufi, A Ormsby, U Raju. Henry Ford Hospital, Detroit, MI.

Background: Sampling error is an expected limitation of CNBX. Triple approach has been successful for fine needle aspiration biopsy of breast lesions. Radiologic pathologic (rad-path) correlation is required for image-guided CNBX (I-CNBX). Actively seeking the imaging and clinical information helps to identify a discordant pathology findings of a highly suspicious clinical and/or radiographic mass.

Design: 673 patients with benign CNBX diagnoses in 2003, performed for clinical and/or radiographic mass-lesions [213 non-image guided (N-CNBX) and 460 I-CNBX] were analyzed for missed cancer. The diagnoses were grouped into 1) specific (SP) for mass lesion (correlated well with a mass; eg. fibroadenoma, papilloma, cyst, nodular sclerosing adenosis, complex sclerosing lesion); and 2) nonspecific (NSP) (uncertain or discordant for mass; eg. stromal fibrosis, fibrocystic change, usual hyperplasia, mild sclerosing adenosis, fibroglandular or fatty breast tissue NOS).

Results: All cases were followed for 6 to 1328 days (mean 826.23). There were 13 missed cancers (1 in SP group, 12 in NSP-group); 4 were I-CNBX and 9 were N-CNBX. By imaging, 5 were birad 5 (highly suspicious), 6 were birad 4 (suspicious); 2 had no imaging. The interval from the benign CNBX to diagnosis of malignancy was 10 days to 9 months. In NSP group (n =220), 109 had I-CNBX and 111 had N-CNBX. Missed cancer rate was highest for N-CNBX if there was also a mass-lesion detected by imaging (7/45); there were no cancer when imaging was negative (0/46). Discordance was recognized and cancer diagnosis was quickly established in 10 patients including all cases of I-CNBX (average 25.88 days ± 14.81 SD), however cancer diagnosis was delayed by > 4 months in 3 N-CNBX cases.

Conclusions: 1). Missed cancer rate is highest for non-image guided CNBX with non-specific benign diagnosis if there is also a mammographic and/or ultrasound mass. 2).The existing rad-path correlation protocols for image-guided CNBX effectively prevent delay in cancer diagnosis. 3). By using triple approach, pathologists and surgeons can recognize possible discordance between the pathologic findings and clinical/ radiologic mass lesion, potentially leading to prompt re-biopsy and definitive diagnosis.

	CNBX	I-CNBX	N-CNBX	Nonsp-group, I-CNBX	Nonsp-group, N-CNBX	Nonsp-group; pos imaging mass, N-CNBX	Nonsp-group; neg imaging, N-CNBX
Total	673	460	213	109	111	45	46
Missed cancer (n)	13	4	9	3	9	7	0
Missed cancer (%)	1.9%	0.8%	4.2%	2.7%	8.1%	15.6%	0

236 Prognostic Significance of EGFR and Phosphorylated EGFR Expression in Invasive Breast Cancer

C Zoubouli, C Magkou, I Giannopoulou, K Karali, S Markaki, E Mylona, L Nakopoulou. Attikon Hospital, Athens, Greece; Medical School, University of Athens, Athens, Greece.

Background: Epidermal growth factor receptor (EGFR) is involved in regulating cell growth in breast carcinomas. Its activated form (pEGFR) is correlated with poor prognosis in lung cancer, whereas it has not yet fully investigated in breast cancer. The aim of this study was to investigate the expression of EGFR, pEGFR and their correlation with overall and disease free survival, clinicopathological parameters (nuclear grade, histological grade, hormonal status, tumor size and stage), the antiapoptotic Bcl-2 and biological markers of invasion and metastasis (uPAR, MMP-9, VEGFR-1/Flt-1).

Design: A three-step immunohistochemical method (ABC/HPR) was applied on paraffin-embedded sections from 156 patients with invasive breast carcinoma to detect the expression of the proteins EGFR, pEGFR, ER, PR, Bcl-2, uPAR, MMP-9 and VEGFR-1/Flt-1. The results were statistically processed using chi-square test. Overall and disease-free survival distribution curves were assessed by Kaplan-Meier test and log-rank statistics followed by Cox's proportional hazards regression model.

Results: EGFR and pEGFR proteins were immunodetected in the membrane of the malignant cells (11.9% and 35.7% respectively), and less commonly in the normal epithelium and in situ component, where they existed. EGFR expression was positively correlated with nuclear grade ($p=0.004$) and negatively correlated with hormonal receptors ER and PR ($p<0.001$ and $p=0.048$, respectively) and bcl-2 ($p=0.008$). pEGFR was positively related to VEGFR-1/Flt-1, uPAR and MMP-9 ($p=0.001$, $p=0.049$ and $p=0.026$, respectively). Univariate analysis showed that only pEGFR-positive cases had poor overall survival ($p=0.017$), a finding that is further supported by multivariate analysis ($p=0.002$).

Conclusions: These data provide clinical evidence that pEGFR expression seems to be an important independent prognostic factor and it is related to angiogenesis and invasiveness. EGFR immunoexpression is related to nuclear grade and hormonal status, and therefore to cellular differentiation.

Cardiovascular

237 Surgical Pathology of Bicuspid Aortic Valve: A 10 Years Survey

C Basso, S Rizzo, A Abudurheman, G Gerosa, G Thiene. University of Padua Medical School, Padua, Italy.

Background: To report the surgical pathology experience on bicuspid aortic valves (BAV) collected in a ten years time interval at a pathology institution serving a single Cardiac Surgery Department.

Design: The medical charts and BAV specimens from patients undergoing aortic valve replacement in the time interval 1994-2003 were retrospectively reviewed. A detailed gross and histologic examination of excised valves was carried out.

Results: Among 1480 pts who underwent aortic valve replacement, 166 pts had BAV (11%). They were 121 M and 45 F, age ranging 1-79 yrs, mean 55±16 (vs 66±12 of the tricuspid aortic valve (TAV) pts, $p<0.0001$). The mean age at operation was 58±15 in BAV pts with aortic stenosis vs 46±15 in BAV pts with pure aortic incompetence ($p=0.0001$). The M/F ratio was 2.7 in BAV vs 1.28 in TAV ($p<0.0001$). 70% of pts presented had stenosis due to dystrophic calcification, 26% had pure incompetence and 4% aortic dissection. Isolated valve replacement was done in 72%, valve replacement plus ascending aorta substitution in 21% and aortic valve replacement plus aortoplasty in 7%. The mean prosthetic diameter was of 24±1.8mm in BAV pts vs 22 ±1.9mm in TAV pts ($p<0.0001$). A raphe was present in 60% of pts. No difference as far as presence of raphe and cusp symmetry was found in stenotic vs incompetent BAV (65% vs 66%, and 66% vs 38%, respectively, p= NS). Pure aortic regurgitation occurred mostly in the setting of aortic root pathology (85%). Overall, infective endocarditis occurred in 6% of BAV pts vs 2% of TAV pts ($p=0.001$). 84 pts were operated due to aortic dissection and a BAV was identified in 8%.

Conclusions: BAV is the underlying substrate of aortic valve dysfunction in 11% of pts requiring surgery, with a strong male predominance. The most common fate of congenitally BAV is stenosis due to dystrophic calcification (70%). Pure aortic incompetence is mostly due to concomitant aortic root pathology. BAV is a not so rare substrate for infective endocarditis and dissection.

238 Endomyocardial Biopsy for In Vivo Diagnosis of Arrhythmogenic Right Ventricular Cardiomyopathy: An In Vitro Validation on Heart Specimens

C Basso, F Ronco, A Abudurheman, G Thiene. University of Padua, Padua, Italy.

Background: Tissue characterization by endomyocardial biopsy (EMB) is a major criterion for in vivo diagnosis of arrhythmogenic right ventricular cardiomyopathy (ARVC). Aim of our study was to assess in vitro the typical histomorphometric parameters in order to define the diagnostic cut-off, sensitivity and specificity of EMB in ARVC.

Design: Sixty heart specimens have been selected: 20 ARVC, 10 dilated cardiomyopathy (DC), 10 controls, 10 adipositas cordis and 10 aged >80 yrs. An in vitro EMB with Cordis disposable bioptome has been performed in the subtricuspid, apex, infundibulum and septum of the RV and in the left ventricular (LV) free wall, for a total of 5 samples per heart. Histomorphometric quantification of the myocardium, fibrous and fatty tissue (percentage of the total EMB area) was performed on Heidenhain thricrome stained slides by Image ProPlus 4.0. Data were compared by ANOVA, and cut-off, sensitivity and specificity were calculated by ROC curves.

Results: The mean residual RV myocardium in the ARVC group was 54,5%± 16,8 ($p<0.001$ vs the other groups), varying from 33,1%±29,8 in subtricuspid, to 33,6%±22,7 in the apex, to 67,4%±21,4 in the infundibulum, to 83,9%±8,9 in the septum. The ARVC diagnostic cut-off was a RV myocardium <64% (sensitivity 80% and specificity 90%). The mean RV fatty tissue in the ARVC group was 16,1%±13,2, with significant differences only vs controls (2,7%±3,6, $p<0,001$) and DC (1,7%±1,9, $p<0,001$), but not vs adipositas cordis group (10,6%± 8,1) and the elderly (7,2%±3,9). The RV fibrous tissue was increased both in ARVC (29,3%±11,5) and in DC (19%±9,4; p=NS).When considering the RV apex sampling site, fatty tissue amount was higher in ARVC (31,9%±26,4) than in DC (4,1%±5,1 $p<0,05$), but no significant differences were found vs controls (10%±15,1), adipositas cordis (30,8%±25,2) and the elderly (26,2 ± 14,3). A diagnostic cut off of RV apex fibrosis>19% (85% sensitivity and 85% specificity) and of RV apex residual myocardium <42% (60% sensitivity and 90% specificity) have been calculated. No significant differences were found among the groups when considering the septum and the LV.

Conclusions: EMB's sensitivity and specificity change accordingly to the sampling site and to the analysed tissue parameter. Fatty tissue is mostly aspecific particularly at the RV apex, whereas the residual myocardium and fibrous tissue appear the most relevant diagnostic parameters. Septal and LV EMB are not useful for diagnostic purposes in ARVC.

239 Risk Factors for Atherosclerosis and the Development of Preatherosclerotic Intimal Hyperplasia

S Bedri, SM Cizek, P Talusan, H Lee, JR Stone. Massachusetts General Hospital, Harvard Medical School, Boston, MA.

Background: Eccentric intimal hyperplasia is considered to be the precursor lesion for atherosclerosis in humans; however, its etiology is unclear. Earlier studies focusing on atherosclerosis-prone arteries have documented preatherosclerotic intimal hyperplasia to be nearly universally well established by young adulthood. To gain insight into the etiology of this process, traditional risk factors for atherosclerosis were correlated with intimal thickness in an atherosclerosis-resistant artery, the internal thoracic artery (ITA).

Design: ITAs from the 2nd intercostal space were obtained from 89 autopsies. Autopsies excluded from the study included those with cardiothoracic surgery, radiation therapy, systemic vasculitis, morbid obesity, and one with advanced atherosclerosis of the ITAs. All ITAs were examined histologically for the presence of atherosclerosis, defined as the presence of multiple foam cells (fatty streaks) or a necrotic/lipid core. Intimal and medial thickness were obtained with a digital camera and SPOT software, and used as the ratio of intimal to medial thickness (I/M). A mean I/M ratio was obtained for each autopsy. The 89 autopsies included 32 women and 57 men, ranging in age from the 3rd to 10th decade of life (median = 62 yrs). A general linear model was used to examine the association between the I/M ratios and risk factors for atherosclerosis: age, gender, hypertension, smoking, body mass index, diabetes, and hypercholesterolemia.

Results: Atherosclerosis was identified in 19 autopsies. The remaining 70 autopsies had no atherosclerosis, and displayed intimal histology ranging from normal to preatherosclerotic intimal hyperplasia. A multivariate analysis of all autopsies revealed only age >75 years to be significantly correlated with atherosclerotic lesion development ($P=0.01$). Multivariate analysis of the I/M ratio in all 89 autopsies revealed age ($P<0.0001$), smoking ($P=0.008$), and hypertension ($P=0.02$) to be significantly correlated with intimal thickness. In the 70 autopsies without atherosclerosis, multivariate analysis revealed the I/M ratio to be independently associated with both age ($P=0.006$) and smoking ($P=0.028$).

Conclusions: Age and smoking were found to be independently associated with the development of preatherosclerotic intimal hyperplasia in the atherosclerosis-resistant ITA of adults. These data suggest that development of preatherosclerotic intimal hyperplasia may be influenced by traditional risk factors for atherosclerosis.

240 Loss of the *PTCH* Gene Locus in Cardiac Fibroma

JA Bridge, M Nelson, M Zhou, R Streblow, V Prasad, C Reyes, D Perry. University of Nebraska Medical Center, Omaha, NE; Arkansas Children's Hospital, Little Rock, AR; Children's Hospital, Omaha, NE.

Background: Cardiac fibroma is a rare benign tumor that is poorly characterized genetically. Mutations of the tumor suppressor gene *PTCH* are the underlying cause of Gorlin syndrome. Cardiac fibroma is seen in 3% of patients with Gorlin syndrome.

Design: Conventional cytogenetic analysis was performed on a peripheral blood and a cardiac fibroma sample from a 2 week old male. In addition, FISH studies were performed to assess the copy number of the *PTCH* gene locus (9q22.3) on metaphase and interphase cells from these same specimens using YAC probe 891G1 and on representative paraffin-embedded tissue sections of two additional cardiac fibromas (one arising in a 2 month old female and the other in a 13 year old male). None of the patients had Gorlin syndrome.

Results: Karyotypically, the following abnormal chromosomal complement was detected in the 2 week old male's cardiac fibroma: 46,XY,del(9)(q22q34)[15]. FISH studies revealed homozygous loss of the *PTCH* locus in the cytogenetically analyzed cardiac fibroma and in the cardiac fibroma arising in the 13 year old male. Heterozygous loss of this locus was identified in the remaining cardiac fibroma from the 2 month old female. A mutational mechanism other than deletion may be responsible for *PTCH* inactivation on the other locus in this latter patient. Conventional cytogenetic and FISH studies of the peripheral blood sample from the 2 week old male were normal.

Conclusions: These data support a tumor suppressor gene role for *PTCH* in sporadic cardiac fibromas.

241 Idiopathic Aortitis of the Thoracic Aorta: Histologic Findings in 55 Cases

AP Burke, F Tavora, N Narula, R Virmani. CVPath Institute, Gaithersburg, MD; Armed Forces Institute of Pathology, Washington, DC; University of California, Irvine, CA.

Background: Aortitis involving the ascending aorta results in aneurysms. The diagnosis of aortitis is often made initially by the pathologist after aneurysm repair. We present a series of 52 cases, with emphasis on histologic features.

Design: 52 cases of aortitis were retrospectively studied with histologic and available clinical information.

Results: There were 42 surgical resections and 10 autopsy specimens. 48 aneurysms involved the ascending aorta alone, and 4 involving the ascending and descending thoracic aorta. No patient had a diagnosis of aortitis prior to surgery or autopsy. There were two histologic types: necrotizing aortitis (NA) and non-necrotizing aortitis (NNA). 43 aortas demonstrated NA, characterized by zonal medial necrosis, surrounded by chronic inflammation, with fibrosis involving the intima and adventitia. In 17 cases of NA with large areas of healing, there was marked accumulation of extracellular matrix. Elderly NA (>60 years) comprised 19 patients, 93% female, age range of 61-85; 12% had acute or chronic dissections. Young NA (<60 years) comprised 24 patients, 50% female, age range 24-55 years, 11% with dissection. Young NA differed significantly from elderly NA (fewer women, p=.002, greater adventitial scarring, p=.007). One elderly patient with NA had a history of temporal arteritis (TA). Two young NA patients had autoimmune disease (Crohn's disease, and lupus erythematosus, respectively); none had a history of Takayasu disease. Subsequent rheumatologic workup on 16 NA patients was negative. Serology for syphilis was negative in all cases. Nine aortas demonstrated non-necrotizing aortitis (NNA), with prominent chronic medial inflammation without necrosis, adventitial fibrosis or significant intimal thickening. There were 6 women, 72 ± 6 years, and 6 dissections. Five had a history of temporal arteritis. NNA patients differed from young NA (more frequent TA, p=<.001, more frequent dissection, p=.02, less adventitial scarring, p<001) and elderly NA (more frequent TA, p=.02, less adventitial scarring, p=.003).

Conclusions: Aortitis is often first diagnosed by the pathologist and cinically unsuspected. NA differs by age < or > 60 years, but is usually isolated without other rheumatologic disease. NNA is associated with temporal arteritis. Healed NA can histologically be mistaken for non-inflammatory medial degenerative disease.

242 Evidence of PVB19 and HHV-6 but Not CMV or EBV Viral Genomes in Archival Cases of Dilated Cardiomyopathy

M Cankovic, C VanBuskirk, J Beher, L Whiteley, RJ Zarbo. Henry Ford Health System, Detroit, MI.

Background: Several studies have suggested that persistence of viral genomes, including those of parvovirus B19 (PVB19), human herpesvirus 6 (HHV-6), human cytomegalovirus (CMV), and Epstein-Barr virus (EBV), among others, may play a pathogenic role in development of dilated cardiomyopathy (DCM). The purpose of this study was to test archival cardiac specimens for the presence of PVB19, HHV-6, CMV and EBV viral genomes to estimate the level of involvement that persistence of viral pathogens might play in pathology of cardiomyopathies.

Design: Archival heart explant and biopsy specimens from 2001 to 2006 were obtained for 60 patients. The cardiomyopathy cases were classified as follows: ischemic (20), dilated (34), hypertrophic (4), and idiopathic (2). Myocardial inflammation was re-assessed by reviewing histological and immunohistochemical analyses. Viral DNA was detected using real time PCR.

Results: PCR amplified viral genomes in 11 of the 60 biopsies. Of these, 7 (11.7%) were positive for HHV-6 and 4 (6.7%) were positive for PVB19. There was no evidence of CMV or EBV viral DNA in any of the biopsies. None of the biopsies showed evidence of multiple viral infections. Of the seven cases positive for HHV-6, two were of ischemic cardiomyopathy, and five of dilated cardiomyopathy. Of the PVB19 positive cases, 3 were diagnosed as dilated cardiomyopathy and one as ischemic cardiomyopathy.

Conclusions: Real time PCR testing of archival endomyocardial tissue for evidence of viral presence is an important tool in the investigation of cardiomyopathy patients. Clinical and experimental observations have demonstrated the ability of viruses to invade, persist, and replicate in the myocardium, where they can induce chronic damage. Our study of this small group of cardiotropic viruses supports other studies which have suggested that myocardial persistence of various viruses may play a role in the pathogenesis of dilated cardiomyopathies. The clinical significance of these findings will be clarified by future molecular studies examining additional viruses in cardiomyopathy tissues compared to autopsy material of normal hearts.

243 C4d as a Marker of Antibody Mediated Rejection in Heart Transplants

SS Daniel, SE Fedson, AN Husain. University of Chicago, Chicago, IL.

Background: Antibody-mediated rejection (AMR) involves antibody deposition in transplant organs subsequently leading to activation of the complement pathway and has been found to correlate with increased risk of graft coronary vasculopathy and lower allograft survival rates. These factors make prompt identification and treatment extremely important. Several pathologic markers have been studied as possible markers of AMR with C4d, a degradation product of the classic complement pathway, being one of the most promising markers since it can be studied both by immunofluorescence and on paraffin embedded tissues. Utility of C4d is already established in kidney transplants, however, there is limited and conflicting data published regarding heart transplants. We analyzed endomyocardial biopsies of heart transplant recipients using C4d as a marker of antibody-mediated rejection.

Design: We prospectively studied 34 consecutive heart transplant recipients from October 2004 to November 2005. Patients received standard triple immunosuppression and routine scheduled endomyocardial biopsies. In addition to H&E stain, IHC stains for C4d were obtained for all biopsies from paraffin-embedded tissues. Cellular rejection was graded using ISHLT criteria. A positive C4d stain was defined as the presence of structural staining without background or serum staining. Positive biopsies were graded for intensity (negative, weak, strong), extent (focal or diffuse) and location (endothelial, interstitial and endocardial). Patient demographics, CMV status of donor and recipient (CMVD/R), hemodynamic data and panel reactive antibodies (PRA) were analyzed by ANOVA and chi-square statistics.

Results: There were 401 biopsies over 6-18 months of follow-up with C4d staining on 394. Twenty biopsies showed positive staining (interstitial 16, endothelial 3, endocardial 1) for C4d. Only CMVD+/R- was associated with positive C4d (p=0.06). Sex, PRA, and hemodynamic function did not correlate.

Conclusions: As with cellular rejection, AMR does not always correlate with hemodynamic dysfunction. Our analysis revealed that positive C4d stains have different staining patterns and intensities, which need to be further studied and correlated with cardiac allograft function over a longer period of time. Thus, pattern, intensity and location of staining should be part of the reporting system for IHC C4d staining.

244 The Mitral Valve Annulus: Revisited

V Dixit, P Vaideeswar, J Butany. University Health Network, Toronto, ON, Canada.

Background: Mitral valve (MV) function is complex and relies on the structural integrity of its components, including the annulus. There is limited literature regarding the morphology of its annulus. This study examines its histo-morphology, and attachments/ orientation.

Design: Mitral valves from twelve human hearts (autopsy or transplant), from patients who had no clinically significant mitral valvular dysfunction, were analyzed. Patient age ranged from 22- 82 yrs, with a male to female ratio of 2:1. The mitral valve, with its atrial and ventricular attachments was serially, longitudinally sectioned and all sections were paraffin embedded. The structure of the valve annulus, including its histologic nature, length, and orientation of the fibrous framework at the annulus were examined. Stains for connective tissue and immunohistochemistry for smooth muscle were performed.

Results: The annulus had a variable structure and appearance. The features described were present in all valves. The annulus was seen as a collagen rich, fibrous annular band (FAB) of variable length, between the left atrium (LA) and the left ventricle (LV), rather than as a complete ring. The length of the FAB varied, as did the orientation of the collagen fibers in it, especially in different parts of the posterior leaflet annulus. The mitral valve leaflets were continuous with the annulus. The collagen in the zona fibrosa of the leaflet and the band was arranged in broad bundles and was continuous. The zona spongiosa (ZS) appears to end at the junction of the leaflet with the FAB in a triangular or wedge shaped spongy core (SC), of loose connective tissue rich in mucopolysaccharides, with microscopic collagen nodules. Furthermore, variable numbers of smooth muscle cells were seen in the proximal third of the posterior leaflet, as were occasional cardiac muscle fibers, in more than 70% of the examined sections.

Conclusions: We conclude that: (1). The mitral annulus is not a ring, but an irregular, tube-like structure of varying length, anchoring the mitral valve, (2). The MV leaflet has smooth muscle cells, suggesting the possibility that its function may have an active component. (3). The MV fibrosa is a continuation of the FAB, and the spongiosa a continuation of the SC of the mitral annulus. (4) This insight into the structure and nature of the FAB may help explain the propensity for mitral annular calcification in the region of the posterior leaflet. (5). Further studies on the valve annulus (FAB) will advance existing knowledge of functional valvular anatomy and the understanding of annular pathologies.

245 Cardiac Myxoma: A Detailed Clinicopathological and Immunohistochemical Study of 39 Cases

D El Demellawy, J Butany. Department of Pathology and Laboratory Medicine, Thunder Bay, ON, Canada; Department of Pathology and Laboratory Medicine, Toronto, ON, Canada.

Background: Cardiac myxomas (CM) are easily diagnosed clinically and usually successfully resected. They are bewildering when it comes to histogenesis.

Design: Thirty nine cases of CM were reviewed and immunohistochemistry performed.

Results: Twenty three cases were females and 16 were males, mean age 54.2 years. Two patients had Carney complex Thirty four cases were located in the left side of interatrial septum , six cases revealed infarction, 5 showed calcification and 3 had ossification . In all cases there were inflammatory cells: lymphocytes(T and B) and macrophages. Immunohistochemical results were consistent in all cases (Table 1).

Conclusions: CM show female, middle aged and left sided interatrial septal predilection. The immunoprofile reveals contribution of neural crest elements, blood vessel endothelium and basement membrane material. The muscle markers were restricted nourishing thick walled vessels' media in CM and myocardium. The cytoplasmic/ membranous expression of beta catenin does not mean that CM is neoplastic, nevertheless, the absence of expression of beta-catenin, calretinin, laminin and CD31 in the myocardium and the recent reports of their expression in the endocardial cushion may suggest the latter as a possible origin of CM. There was no difference in CM immunoprofile in the setting of Carney complex.

TABLE 1

Origin Expression	Mesothelial/ Neural Crest	Mesothelial	Mesothelial/ Lymphatic Endothelium	Blood Vessel Endothelium	Basement Membrane	Basement membrane, Muscle	Wnt/ Beta-Catenin Pathway
Markers' Expression	Calretinin : (+) Diffuse Nuclear & Cytoplasmic Calretinin : (+) Diffuse Nuclear & Cytoplasmic	CK5,6, WT-1 & HBME-1	D2-40: Cytoplasmic	CD31: Granular, Membranous	Laminin: Cytoplasmic	Collagen IV, MSA, Colponin: Cytoplamic	Beta-Catenin: Granular, Cytoplasmic & Membranous
Myxoma Cells	+	-	-	+/F*	+	-	+
Vasoformative Channels	+	-	-	+/F*	+	-	+
Endothelium	-	-	-	+	+	-	+
Nourshing Vessels	-	-	-	-	-	+	-
Capillaries/ Lymphatics	-	-	+	+	-	-	+
Myocardium	-	-	-	-	-	-	-
Intercalated Discs	-	-	-	-	-	-	+
Adipose Tissue	+	-	-	-	-	-	-

*F= focal. MSA: Muscle Specific actin. S100 & HEPAR-1 were (-) in all except for adipose tissue in the former.

246 β-Catenin and Connexin 43 Remodeling at the Intercalated Discs in End-Stage Cardiac Hypertrophy

P Francalanci, A Tessa, R Boldrini, C D'Anna, S Lucioli, R Mariani, FM Santorelli, F Callea. Bambino Gesù Children's Hospital, Rome, Italy.

Background: Cardiac hypertrophy, primitive as well as acquired, is characterized by an increased protein synthesis, cellular sized and disarray of myocells with subsequent remodeling of intercalated discs (ID). Whereas electrical signals and small molecules are exchanged in gap junctions (GJ) mainly composed of connexin 43 (Cx43) and 45, mechanical forces are transduced longitudinally between adjacent cells through fascia adherents (FA) and desmosomes junctions. In FA, barb end of actin of terminal sarcomeres links N-cadherin through binding to α-catenin, which sequentially connects to β- or γ-catenin. Previous study showed that β-catenin accumulates at ID in hamster and human primitive hypertrophic cardiomyopathy (HCM), hypothesizing that this deposit contributed to sarcoplasma stiffness and alteration of the electrical exchanges in HCM. β-catenin metabolism is regulated through release of Wnt1 or Ser-9 phosphorylation of GSK-3β.

Design: To evaluate the ID remodeling in acquired cardiac hypertrophy and to estimate expression of cadherin/catenin complex in AJ as well as of connexin 43 (Cx43) in GJ, 23 children (aged 1-15 years) with dilated cardiomyopathy (DCM) and 13 children (aged 9-24 years) with congenital heart disease (CHD), were studied by light and electron microscopy, immunohistochemistry and Western blot analysis.

Results: Hypertrophic and disarrayed myocells and IDs were evident in all samples. In disarrayed ID, β-catenin immunostaining was increased and fragmented in all samples. Cx43 expression was abnormal in all, showing a distribution over the entire surface of the myocytes, consistent with fetal distribution. By Western blotting analysis, β-catenin was significantly increased in DCM (+43%) and in CHD (+42%). Contrariwise, Cx43 was normal. In hypertrophied heart, high β-catenin levels occurred in the face of unchanged amount of Wnt1 and low amount of SGK-3β.

Conclusions: This study suggests that β-catenin deposits occur at the AJ in end-stage hypertrophic ventricular myocytes, regardless of either primitive or acquired hypertrophy. A GSK-3β decrease implies an elevated β-catenin stability rather than increased protein synthesis. Remodeling of adhesions junctions does not lead to a quantitative change of Cx43. Its abnormal expression, mimicking fetal phenotype during eutrophic hypertrophy of cardiomyocytes, suggests some sort of reactivation of an early gene program.

247 Minocycline Is as Effective as Statin Therapy in Resolution of Metalloproteinase Expression in Atherosclerosis

A Fujimoto, J Zhou, S Fujimoto, A Petorov, Y Matsumoto, R Doshi, K Miki, T Ishii, N Narula, J Narula. University of California, Irvine, Irvine, CA; Toho University, Tokyo, Japan.

Background: We evaluated the role of anti-inflammatory, anti-apoptotic anti-biotic, minocycline, administration on plaque characteristics.

Design: Atherosclerosis was produced in 35 NZW rabbits by balloon deendothelialization and hypercholesterolemic diet for 4 months; 12 unmanipulated rabbits on normal chow were used as controls. In the last month, 6 of the 35 atherosclerotic rabbits received normal chow, 6 fluvastatin (1mg/kg), and 5 received minocycline (3mg/kg) once a day. Explanted aortic segments were stained with Movat pentachrome, MMP-1, 2, 3, 8, 9, macrophage (RAM-11), smooth muscle cells (SMC, α-actin). Percent immunopositive areas were calculated for RAM-11, α-actin and MMP 1, 3, 9. TUNEL was performed for identification of apoptosis in neointima.

Results: Minocycline reduced macrophage content and MMP 1,3,9 expression (1.3%±0.9, 0.1%±0.07, 0.095%±0.03, 0.09%±0.03, respectively) significantly compared to continuous diet group (3.3%±1.6, 0.3%±0.07, 0.2%±0.06, 0.1%±0.08, respectively) and as effective as statin therapy (1.9%±0.9, 0.18%±0.07, 0.1%±0.05, 0.08%±0.05, respectively). TUNEL positivity also resolved significantly in minocycline group. SMC prevalence increased significantly by minocycline.
Conclusions: Our results demonstrate that minocycline is as effective as clinically favorable interventions (dietary modification and statin therapy) in reolution of MMP expression and stabilization of plaques, and suggests a role for additional anti-inflammatory therapy.

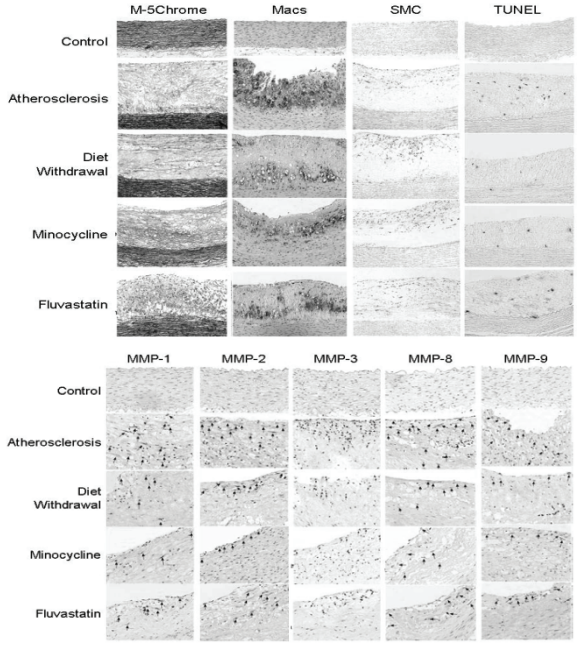

248 Primary Cardiac Angiosarcoma (CA): A Clinicopathologic Analysis of Five Cases

Y Ge, D Kim, CH Kim, J Zhai, MJ Reardon, D Coffey, AG Ayala, JY Ro. Methodist Hospital, Houston, TX; Korea University, Seoul, Korea.
Background: Although primary CA is rare, it is the most common malignant neoplasm of the heart in adults. Therefore, we analyzed the clinicopathologic characteristics of five patients with this disease who were seen and treated at one institution over the past seven years.
Design: Tissue microarray slides were prepared from representative tissue blocks for routine hematoxylin and eosin and immunohistochemical (IHC) stains including CD31, CD34, FLI-1, cytokeratin (CK), D2-40, HHV8, EGFR, p53 and Ki67.
Results: There were 3 males and 2 females, with a mean age of 40.6 (20-61) years. The most common presenting symptom was dyspnea. Local tumor extension (4/5) and distant metastasis (2/5) were common at the time of diagnosis. All tumors were located in the right atrium and had an average tumor size of 8.0 (3.7-13) cm. Tumors were hemorrhagic with variegated tan-brown solid areas. Histologically, they exhibited high-grade morphology with focal areas resembling Kaposi's sarcoma. The cells were epithelioid or spindle and there was frequent hemorrhage and necrosis. On IHC study, the tumor cells were strongly positive for CD 31, CD 34 and FLI-1, but were negative for CK, D2-40, HHV8 and EGFR. Furthermore, the tumor cells were frequently positive for p53 (4/5) and for Ki-67. In none of the patients a complete tumor resection could be done due the large tumor size, ventricular extension, or extensive pericardial involvement. All patients received pre- or post-surgical chemotherapy. Four of the patients survived from 1 to 11 (mean 6) months after diagnosis. One patient has survived 58 months in spite of multiple local recurrences and metastasis.
Conclusions: CAs are rare tumors with predilection for the right atrium. They exhibit an anaplastic histology with a high proliferative rate on Ki-67 and often display p53 expression. Although these tumors may resemble Kaposi's sarcoma, there is no evidence that HHV 8 is involved. Although surgery remains the essential modality of treatment, resection is often incomplete and the prognosis is poor. The relatively long survival of one of our patients did not correlate with tumor size, location, histological grade, growth pattern, IHC profile, or margin status.

249 Detecting Acute Infarction in Autopsy Myocardium. Is There a Better Way Than Hematoxylin and Eosin (H&E)?

M Guzman, F Desoto-Lapaix, M Pincus, R Wieczorek. VA New York Harbor Healthcare System-Brooklyn Campus, Brooklyn, NY; SUNY-Downstate Medical Center, Brooklyn, NY.
Background: Detecting an acute myocardial infarction in autopsy myocardium prior to neutophilic infiltration is often very subtle on H&E. Areas of wavy fibers, and loss of cross striations may be easily missed especially if they are small. Massons trichrome stain may be used to differentiate necrotic myocardium (blue cytoplasm) from viable myocardium (red cytoplasm) often with a borderline of purple myocardial cytoplasm surrounding a necrotic area, but the results are dependent on which method is used. Desmin is a cytoplasmic intermediate filament protein involved in mitochondrial positioning and respiratory function in the myocardium and skeletal muscle. In experimental models, in myocardial ischemia, desmin shows degradative changes from 30 minutes to 2 hours of the ischemic insult. This study was undertaken to see if loss of desmin can be used as a marker for early acute myocardial infarction, and to compare it to conventional H&E and Massons trichrome stains.
Design: 18 autopsy cases of acute myocardial infarction (documented by serum, ECG, or gross evidence), with infarcts ranging in age from less than 12 hours to 24-48 hours, were stained with Desmin (D33) in a 2 step immunoperoxiodase method with DAB, Massons trichrome, and H&E stain. Intensity of cytoplasmic immunostaining was graded as 0 negative, 1+ light tan, 2+ dark tan, and 3 + entirely dark brown.
Results: In all cases, the myocardial cytoplasm of the acutely infarcted areas was negative on desmin stain, and deeply blue on Massons trichrome stain. Viable myocardium of all cases was 3 + on desmin, and red on Massons trichrome stain. The borderline areas around an acute infarction of all cases were 1 to 2 + with desmin, but the same borderline areas on Massons trichrome in 5/18 (28 %) were red with the remaining showing a purple color. Comparing the desmin stain to the H&E stain in all cases, the negative immunostaining allowed an easier discrimination of an acute infarction with its tan border and surrounding viable dark brown myocardium, than the H&E, which had a subtle deeper eosinophilic color in an acute infarct as compared to viable myocardium. Borderline areas were very difficult to discern on the H&E stain as compared to desmin.
Conclusions: We conclude that the desmin immunostain is a more sensitive way to detect early acute myocardial infarction than Massons trichrome stain or the H&E stain.

250 Idiopathic and Non-Idiopathic Giant Cell Aortitis: A Clinicopathological Study of 43 Cases

S Lantuejoul, A Barbour, E Brambilla, AG Nicholson, MN Sheppard. CHU Michallon, INSERM U578, Grenoble, France; University of Adelaide, Adelaide, Australia; Royal Brompton Hospital, London, United Kingdom.
Background: Giant cell aortitis is classically reported in association with connective tissue or infectious diseases, but can be coincidentally encountered.
Design: In order to depict the clinicopathologic features of giant cell aortitis, we have analysed 43 specimens from 28 patients with idiopathic and 15 with non-idiopathic giant cell aortitis.
Results: For patients with non- idiopathic giant cell aortitis (12F: 3M, av. age = 66 yrs) related to collagen vascular diseases (n=5), temporal arteritis (n=3), rheumatic fever (n=3), Takayasu disease (n=1), syphilis (n=2), and tuberculosis (n=1), aorta was removed for anevrysm (n=11), dissection (n=2), or valve replacement (n=2). Patients with idiopathic giant cell aortitis (20F: 8M, av. age =59 yrs) presented aortic anevrysm (n=22) or dissection (n=6). In both idiopathic and non-idiopathic giant cell aortitis, intima and adventitia were moderately fibrosed with mixed inflammatory cells. Atheroma was found in 9/43 cases and media myxoid changes in 6/43. Quadrangular eosinophilic collagen necrosis, surrounded by giant cells, lymphocytes, plasma cells and some neutrophiles, was found in the media in 11/15 (73%) non- idiopathic and 24/28 (85%) idiopathic giant cell aortitis, respectively. No definitive histological criteria was found to distinguish between these two conditions.
Conclusions: Giant cell aortitis is predominantly found in middle-aged females presenting aortic anevrysm, with idiopathic predominating over those associated with previous disease. While dissection is far more frequent in idiopathic giant cell aortitis, aortic valve involvement is more prominent in those associated with previous disease.

251 Mitral Valve Repair: Causes of Failure

A Luk, J Butany, A Jegatheeswaran. University Health Network, Toronto, ON, Canada.
Background: Mitral valve (MV) repair is today,the surgery of choice in patients with mitral regurgitation. This study reviews the histological features of excised mitral leaflets and annuloplasty rings of patients who had previous MV repair or attempted repair.
Design: 54 surgically excised MV leaflets and 39 annuloplasty rings, excised over 15-years at one institution were reviewed. Patients were separated into groups based on the time interval between surgeries: attempted repair, <30 days, 30-365 days and >1 year. The tissue was examined in detail to determine the causes of mitral valve repair failure and to document the changes in the tissues.
Results: The fifty-four patients had a mean age of 55.7 $\pm$ 17.9 years at the time of surgery after failed repair or attempted repair, of the MV. Index surgery for all patients had been performed between 1973 and 2005. The interval between index surgery and readmission (n=49, 91%, excluding those with MVR following attempted repair) was 6.61 $\pm$ 7.12 years. Myxomatous change and infective endocarditis (IE) were the cause for failure of attempted MV repair. Non-valvular causes(ischemia, chordal rupture and flow abnormalities) and acquired changes, degenerative change, myxomatous change and IE were causes for repair failure in patients at <30 days post-operatively. Degenerative changes (myxomatous and rheumatic[RD}) were the main underlying pathology for failed repair between 31-365 days. At over 1 year after original surgery, repairs failed due to degenerative (myxomatous, RD) and IE and non-valvular (ischemia and chordal rupture) causes.
Conclusions: Although MV repair is the preferred treatment for mitral regurgitation, failure of repair may occur in a relatively small percentage of patients, at the time of surgery or over varying periods after surgery. The failure of repair may be due to IE, significant fibrosis, calcification and nodular thickening at and around the operative site, thickening and stiffening of the synthetic chordae tendinae due to tissue overgrowth, rupture of chordae tendinae, and progression of acquired degenerative disease. All of these lead to recurrence of symptoms of mitral valve dysfunction, and valve replacement surgery.

252 A Pathologic Study of 1606 Surgically Excised Aortic Valves and Concomitant Cardiovascular Tissues

JH Ma, BK Chiu. University of Alberta, Edmonton, AB, Canada.

Background: The relative frequency of pathologies identified in aortic valve (AV) resection specimens has shown substantial change over time, fibrocalcific changes now being most commonly seen. These pathologic processes are not restricted to the AV but may affect other cardiovascular tissues as well. The present study examines the pathology of AV and concomitantly resected cardiovascular tissues.

Design: The pathology of surgically removed AV and concomitantly resected tissues over a 10-year-period at a tertiary-care centre was reviewed. Each patient's clinical history was obtained using the netCARE (Capital Health Electronic Health Record System).

Results: Among 1606 excised AV (mean age 67, range 14-89, female to male ratio 1:2), degenerative valves with fibrocalcific changes (calcific aortic stenosis, CAS) were seen most frequently (n=1041, 65% of total AV, mean age 71; stenotic and/or regurgitant n=1007, 97% of fibrocalcific AV) and commonly associated with major cardiac risk factors and cardiovascular co-morbidities, such as coronary artery disease/aorto-coronary bypass surgeries, ascending aortic dilatation and dissection. The calcific and remodeling processes also affected the adjacent structures, causing calcification of the mitral annulus and the subaortic ventricular septum, necessitating mitral valve replacement (n=63) and septal myomectomy (n=36). Congenitally abnormal valves were seen in 243 AV (15%); these were frequently bicuspid (BAV n=234, age range 14-72, mean age 52) with fibrocalcific stenosis (n=198, 81% BAV). The calcification process was seen early in young patients. BAV were also associated with other cardiovascular abnormalities (aortic coarctation n=5, dilation n=27, dissection n=1). Post-inflammatory changes due to chronic rheumatic disease were seen in 108 AV (6.7% of total, mean age 58 years, stenotic and/or regurgitant n=99, 92% of AV with post-inflammatory changes), with 72 cases simultaneously affecting the mitral valve. Infective endocarditis was seen in 68 cases (4.2%) and associated with intravenous drug abuse, n=7, BAV n=8, and aortic coarctation, n=1. Degenerative valves related to myxomatous changes with valvular incompetence were seen in 95 AV, including 10 cases with Marfan's syndrome.

Conclusions: This study confirms the relative frequencies of pathologies in resected AV specimens in recent years. It also documents associated changes in adjacent cardiovascular tissues and relates relevant clinical information to AV pathology. That AV pathologies are not isolated diseases has important therapeutic implications.

253 Expression of the Cartilage Specific Proteins in the Atherosclerotic Arteries

M Moghadamfalahi, F Galiano, K Doege. LSUHSC, Shreveport, LA.

Background: It is believed that vascular smooth muscle cells (VSMCs) undergo chondrogenic commitment eventually leading to vascular calcification, by mechanisms similar to those governing ossification in the cartilage growth plate.

Design: We examined sections from a total of 27 cases of normal or atherosclerotic coronary and extremity arteries. Sections from 2 normal, 1 atherosclerotic and 3 calcified atherosclerotic coronary arteries from 6 autopsy cases were selected for in situ hybridization analysis. In addition, sections from extremity amputation specimens were included in the study: 1 normal, 1 calcified atherosclerotic, and 1 calcified atherosclerotic with osseous metaplasia of extremity arteries. 3 sections from each sample were examined for aggrecan, collagen II and collagen X expression by insitu hybridization using radioactively labeled antisense RNA probes. Controls included human and mouse cartilage sections, as well as sense cRNA probes.

Results: Control sections of the human and mouse cartilage were strongly positive for aggrecan, collagen II. There were strong signals in the medial (muscularis) layer of the atherosclerotic and calcified atherosclerotic coronary and extremity arteries for aggrecan and collagen II. Areas with the positive signals were comparable in the sections of the arteries, with the stronger reactivity in the calcified areas. Normal sections were negative for the cartilage transcripts. Collagen X did not produce any signals, possibly because collagen X is a transient marker that is expressed during the transformation of cartilage to bone.

Conclusions: Advanced atherosclerotic lesions exhibited areas, which were expressing the cartilage specific genes collagen II and aggrecan. The results suggest that cartilage-associated proteins may be involved in the pathogenesis of atherosclerosis. Considering the high prevalence of the atherosclerotic cardiovascular diseases and being number one killer in U.S, this finding may help us to develop a new treatment method for the arterial atherosclerotic diseases at the molecular level.

254 Octanediol Treatment of Glutaraldehyde Fixed Bovine Pericardium: Sharp Evidence of Anticalcifcation Efficacy in the Subcutaneous Rat Model

E Pettenazzo, M Valente, G Thiene. University of Padua Medical School, Padua, Italy.

Background: Anti-calcification strategies in glutaraldehyde-(GA)-fixed xenograft tissue aim to extract lipids or to neutralize toxic aldehyde residuals. The purpose of this study was to evaluate the efficacy of octanediol (ON) anti-calcification treatment of GA-fixed bovine pericardium (BP), compared to standard (ST) GA-fixed BP. ON-treatment is an ethanolic solution containing a long chain aliphatic alcohol (5% 1,2-octanediol) which removes lipids without diminishing the stability of GA-fixed collagen.

Design: ON and ST-treated BP were both implanted in 24 Sprague Dawley rats, explanted after 30-75 days (12 animals each) and submitted to x-ray, histology (score 0-4 mineralization), electron microscopy (EM) and atomic absorption spectroscopy. Unimplanted ON and ST-treated BP served as control.

Results: Figure shows the mean values of calcium content. At 30 days ON-treated BP disclosed absent calcification vs 20.07 ± 36.79 mg/g dry weight for ST-BP. The difference was sharply evident at 75 days: mean calcium content of 2.36 ± 7.38 mg/g dry weight for ON vs 165.61 ± 23.35 mg/g dry weight for ST ($p < 0.0001$). Striking differences were also detected at histology (mean score 0.3 ± 0.9 ON vs 3.6 ± 0.7 ST at 75 days). At EM collagen appeared well preserved regardless type of treatment. In ON-treated pericardium cell membranes disappeared and only few small profiles of endoplasmic reticulum and rare mitochondria were visible.

Conclusions: Treatment with ON strongly prevents BP calcification in rat subdermal model even in the long-term. Clear-cut evidence of ON efficacy may entail important implication in the development of new generation bioprosthetic valves.

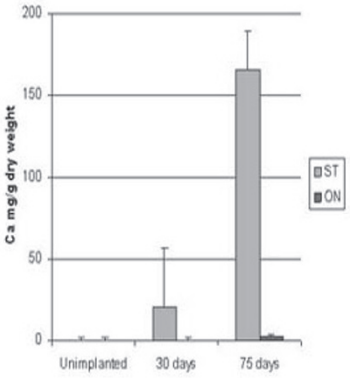

255 Non-Coronary Causes of Sudden Cardiac Death – Experience from a UK National Referral Centre over a Twelve Year Period

SMH Rizvi, A Fabre, MN Sheppard. Royal Brompton Hospital, London, United Kingdom.

Background: Sudden cardiac death is a significant cause of mortality, the majority of these are due to ischaemic heart disease. As a national referral centre for cardiac pathology, we see a significant number of cases of non-ischaemic cardiac sudden deaths.

Design: A total of 710 cases of sudden cardiac death in males (n=449) and females (n=261), referred during 1994-2006 (inclusive) were retrieved from the archives after excluding ischaemic heart disease. These were reviewed and categorised as morphologically normal heart, cardiomyopathies (CMPs) including arrhythmogenic ventricular dysplasia(AVD), dilated cardiomyopathy (DCM), hypertrophic cardiomyopathy (HOCM) and secondary cardiomyopathy, cardiac hypertrophy/fibrosis (idiopathic left ventricular hypertrophy, left ventricular, septal and biventricular hypertrophy and fibrosis), myocarditis (lymphocytic, giant cell, toxic or other), sarcoidosis, valvular defects, non-atheromatous coronary anomalies (abnormal anatomic origin or course, bridging, dissection, and vasculitis), congenital heart disease (CHD) and other causes.

Results: Of the total cases, 357 (50%) did not show any macroscopic or microscopic abnormality. There were 110 cases with CMP (16%), 108 with myocardial abnormality (15%) which comprised both myocardial hypertrophy (n=98) and fibrosis (n=10). Myocarditis was present in 41 cases (6%), valvular defects in 25 cases (3.5%), coronary abnormalities in 24 cases (3.4%), CHD was present in 10 cases (>1%) and other abnormalities in 35 cases (5%). The other causes included Sarcoidosis (n=13, <2%), Fabry's disease (n=3, <1%), Amyloidosis (n=1), Tuberous Sclerosis with multiple ventricular lipomata and lipoma of AV node (n=1), Mesothelioma involving AV node, (n=1), fibrosis of AV node (n=2), microthrombosis with microinfarcts in idiopathic thrombocytopaenic and thrombotic thrombocytopaenic purpura (ITP and TTP, n=1 each, <1%), aneurysm of the membranous septum (n=1<0.5%) and Libman-Sacks endocarditis (n=1), known Wolff Parkinson White syndrome with features of HOCM (n=2, <1%), atrial infarct with haemopericardium and normal coronaries (n=1, <0.5%) amongst other causes (n=7).

Conclusions: Our data emphasizes the morphologically normal heart in sudden cardiac death which points to the role of channelopathies. In addition the role of cardiomyopathies is also highlighted with the emergence of idiopathic left ventricular hypertrophy and fibrosis in which further studies are needed including family history and genetic analysis.

256 Temporal Evolution of C4d Deposition in Antibody Mediated Cardiac Allograft Rejection

AC Roden, BS Edwards, HD Tazelaar, WD Edwards, MC Aubry, DV Miller. Mayo Clinic, Rochester, MN; Mayo Clinic, Scottsdale, AZ.

Background: Deposition of C4d has been proposed as a marker of antibody mediated rejection (AMR) of solid organ transplants. The temporal evolution of initial C4d binding to endothelial cells to its clearing has not been well studied in cardiac allografts (CA), in part because recognition of AMR is elusive (histopathologic criteria are not entirely specific or sensitive). In this study C4d deposition in endomyocardial biopsies (EMB) was evaluated longitudinally from CA recipients clinically suspected of having AMR.

Design: CA recipients suspected of having AMR (on the basis of heart failure early in the post-transplant course that did not respond to increased immunosuppression and was not due to infection) were identified by retrospective chart review. EMB from the first postoperative week, and during any subsequent clinical rejection episodes were stained with H&E and C4d (immunoperoxidase stain, Alpco Diagnostics, Salem, NH). When positive staining for C4d was observed, additional EMB taken from 4 weeks prior to and 12 weeks following the positive EMB were stained. The intensity of capillary endothelial C4d staining was classified as negative, equivocal, when it was focal or weakly positive and positive when all capillaries showed strong staining.

Results: The study group comprised 13 cases with a total of 146 EMB. One patient had positive staining in a single initial EMB (2 days post-transplant). There were no EMB taken prior to this and subsequent EMB remained positive to 9 weeks. Selected EMB from between 3 months to 12 years thereafter were all negative. EMB from 2 patients had equivocal staining (7days and 4 weeks post-transplant, respectively). There were no biopsies taken prior to this. Subsequent EMB from both showed resolution within 3-5 weeks. All other EMB were negative.
Conclusions: Positive C4d staining is uncommon even among patients manifesting clinical features suspicious for AMR; only 1 of 13 such patients had positive C4d staining. C4d was detected as early as 2 days post-transplant and can persist for 9 weeks before being completely cleared. These findings indicate that immunoperoxidase staining for C4d may not be as sensitive a marker for AMR in the heart as it seems to be in other solid organ transplants.

257 Sensory Innervation in Human Myxomatous Mitral Valves: Evidence from Expression of Target Derived Neurotrophic Factors

ER Rodriguez, BP Griffin, CD Tan. Cleveland Clinic, Cleveland, OH.
Background: The innervation of the human atrioventricular valves has been described showing an intricate network of nerve fibers that extend from the base to the free border of the leaflet. The role of these nerve fiber networks is said to be in aiding contractility of the valve. However the cellularity of human atrioventricular valves is predominantly endothelial cells, fibroblasts and some myofibroblasts. Rare smooth muscles cells are present. Cardiac myocytes are sparingly present at the interface of the atrium and fibrous annulus at the base of the valve, thus it is unlikely that they contribute in any significant manner to contractility of the leaflet. Characterization of the target derived neurotrophic factors produced in the human mitral valve and their receptors may provide information about the function of the nerve fibers that populate these leaflets.
Design: Normal (n=4) and myxomatous (n=4) human mitral valve leaflets were immunostained with antibodies to: nerve growth factor (NFG), brain derived neurotrophic factor (BDNF), neurotrophins 3 and 4 (NT3) and (NT4) and their receptors TrkA, TrkB and TrkC as well as vasoactive intestinal polypeptide (VIP). Quantitation of mRNA expression of these neurotrophins was performed by real time polymerase chain reaction (RT-PCR).
Results: All valves showed expression of the neurotrophins BDNF, NT3 and NT4, the neurotrophin receptor TrkB and VIP by immunohistochemistry. Their distribution is located mainly in the valvular interstitial cells present in the spongiosa. To a lesser extent, they are also present in the fibrosa and the atrialis. The myxomatous valves show a much more prominent expression of these markers that the normal valves. RT-PCR showed higher expression of NT3, TrkB, TrkA and VIP mRNA in the myxomatous valves.
Conclusions: The expression of neurotrophins and their receptors in the mitral valves suggest that the innervation of the valve may be sensory rather than motor. Similar sensory networks have been demonstrated in the baroreceptors of the aorta. The increased expression of these molecules in the myxomatous valves may indicate that there is a dysregulation of the sensory function of the myxomatous valves.

258 Expression Profiling of Normal and Myxomatous Human Mitral Valves

ER Rodriguez, BP Griffin, CD Tan. Cleveland Clinic, Cleveland, OH.
Background: Mitral valve prolapse (MVP) is the most common cause of severe non-ischemic mitral regurgitation in the USA. The pathology of MVP affects the 3 layers of the valve (atrialis, spongiosa and fibrosa) as well as the chordae tendineae. Studies of the composition of the valve leaflets in MVP have shown an increase of glycosaminoglycans (hyaluronan, chondroitin, and dermatan sulfate), predominantly in the spongiosa, which weakens the valve. The origin of this increase is unknown. The cells responsible for this increase are thought to be interstitial cells. However there is no knowledge of the gene expression of human mitral valve or valves from patients with MVP.
Design: Normal (n=4) and myxomatous (n=4) human mitral valve leaflets were obtained at the time of MVP surgery or from explanted human hearts without MVP. Total RNA was extracted and cDNA was synthesized. Two-color expression microarrays (Agilent) with 22,000 features were run using dye swap replicates to verify expression levels. The microarray data sets were analyzed using GeneSpring v.7.3 (Agilent). Real time polymerase chain reaction (RT-PCR) was used to verify the expression of some of the transcripts. Immunoperoxidase was used to localize the gene product in the tissues.
Results: Gene sets involved in the synthesis and degradation of glycosaminoglycans (hyaluronate, dermatan, keratan sulfate and iduronate), collagens (X and XXIII), matrix metallopeptidases, and bone morphogenetic proteins were upregulated in the MVP samples with respect to normal. Other genes showing differential expression between normal and MVP included some target-derived neurotrophic factors and their receptors. RT-PCR confirmed the overxpression of the transcripts that showed upregulation in the microarrays.
Conclusions: Gene expression analysis is a useful tool to understand the biology of the normal human mitral valve and to address pathologic states of the mitral valve. Particularly we show that there are specific differences in the synthetic and catabolic pathways during the turnover of the normal mitral valve stroma and that these pathways are differentially regulated in mitral valve prolapse.

259 Utility of Immunofluorescence and Electron Microscopy in Endomyocardial Biopsies from Patients with Unexplained Heart Failure

RC She, EH Hammond. University of Utah Health Sciences Center, Salt Lake City, UT; LDS Hospital, Salt Lake City, UT.
Background: Dallas criteria relevance in defining myocarditis has come into question due to its low sensitivity, its lack of correlation with treatment outcomes, and a newer understanding of viral and autoimmune heart disease. Immunofluorescence (IF) detection of immune reactants is a useful method to detect autoimmune phenomena in tissues. Electron microscopy (EM) allows better visualization of changes within the vasculature and myocytes which may potentially add diagnostic and prognostic information.
Design: This was a retrospective descriptive study of pathology records of native endomyocardial biopsies (EMBX) performed 1981-2006. Biopsies were taken from patients with decreased cardiac function in the presence of normal coronary angiographic studies. Light microscopy (LM) identified cases as satisfying Dallas Criteria (Dallas+), borderline, persistent, or resolving myocarditis (Dallas+/-), or cardiomyopathy (Dallas-). IF studies (HLA-DR, IgG, IgM, IgA, C3d, C1q, and fibrin) examined for interstitial, capillary, or heart-reactive antibody (HRA)-like staining patterns. EM identified cases with capillary endothelial changes and myofilament loss.
Results: 474 records from 429 individual patients (age 6 mo - 78 yr) were identified, 443 of which included EM. Active myocarditis (Dallas+) accounted for 44 cases. Significant IF and/or EM findings were identified in 421 cases:

Table 1

	LM Dallas+	LM Dallas+/-	LM Dallas-	Total
IF+ capillary	19	18	124	161
IF+ interstitial only	14	13	51	78
IF HRA-like+ only	1	2	8	11
IF HLA-DR+ only	7	9	55	71
IF-	3	7	143	153
Total	44	49	381	474

Table 2

	LM Dallas+	LM Dallas+/-	LM Dallas-	Total
EM capillary changes	22	32	168	222
EM myofilament loss	14	26	205	245
EM non-specific findings	10	3	68	81
EM no pathology	1	1	23	25

Conclusions: Most EMBX showed evidence of significant immune-related heart disease not demonstrable by LM, suggesting that IF is a useful strategy on EMBX to define autoimmune phenomena. EM contributed additional information about myofilament loss, a finding which has been reported to correlate with adverse clinical outcome. The frozen tissue from the IF will be used in future studies to characterize viral and autoimmune molecular profile of the tissues. We recommend that all EMBX routinely save tissue for IF and EM.

260 Cardiomyopathy with Glycogen Storage Phenotype Shows Mutations in 2.6% of Heart Transplant Patients at the Cleveland Clinic

CD Tan, NR Friedman, RC Starling, ER Rodriguez. Cleveland Clinic, Cleveland, OH.
Background: The classification of cardiomyopathies is rapidly evolving because of advances in molecular testing. Glycogen storage disease typically presenting as hypertrophic cardiomyopathy is reported to be caused by mutations in two genes that encode the γ-2 regulatory subunit of AMP-activated protein kinase (PRKAG2) and lysosome-associated membrane protein 2 (LAMP2). We describe 3 patients who underwent cardiac transplantation with mutations in PRKAG2 and LAMP2 presenting as dilated cardiomyopathy.
Design: Routine examination of explanted hearts from January 2005 to June 2006 (n = 112) identified 7 cases (6.25%) with light microscopic findings suggestive of a metabolic problem. An eighth case was identified retrospectively because she was the mother of one of the patients with abnormal histology and she also had a heart transplant. Genomic DNA was extracted from frozen tissue of the explanted hearts. The coding sequences of PRKAG2 and LAMP2 genes were amplified by polymerase chain reaction and both strands directly sequenced to screen for mutations.
Results: Only 3 of the 8 patients had significant mutations in the coding regions of either of these 2 genes. The first patient was a 12 year old boy with acute, refractory heart failure whose explanted heart showed marked vacuolation of myocytes. It was discovered that his mother had also been transplanted 7 years earlier at age 32 for "viral myocarditis". The third patient was a 48 year old female whose symptoms started six years earlier with heart failure and tachyarrhythmias. Gross examination of explanted hearts showed cardiomegaly with biventricular dilatation. The third patient also showed patchy areas of transmural fibrosis in the left and right ventricles. Marked myocyte hypertrophy with vacuolated cytoplasm and severe fibrosis were prominent on histology. A G274A mutation in the LAMP2 gene resulting in a stop codon Trp46X is present in the mother and son. A C1810A missense mutation in the PRKAG2 gene leading to a Thr400Asn substitution is present in the third patient.
Conclusions: A variable disease onset and dilated cardiomyopathy phenotype can be seen in glycogen storage diseases. The diagnosis can be suspected on light microscopy. Genetic testing of cardiomyopathy in young adults can ascertain the diagnosis and allow for screening and genetic counseling of family members.

261 Cardiac Transplantation for Giant Cell Myocarditis: The Cleveland Clinic Experience

CD Tan, ER Rodriguez. Cleveland Clinic, Cleveland, OH.
Background: Cardiac transplantation is an accepted primary therapy for giant cell myocarditis (GCM). Recurrence in the transplanted heart is a known phenomenon. The multicenter Giant Cell Myocarditis Registry reported a recurrence rate of 26% at a mean of 3 years posttransplantation.
Design: Since 1984, there were 1251 heart transplant recipients at the Cleveland Clinic. Of these, 7 patients were diagnosed with GCM and had a mean follow-up period of 5.5 years (range 2 to 9 years). The clinical course and outcome in these patients are described.
Results: There were 5 females and 2 males whose age ranged from 28 to 55 at the time of transplantation. Two patients received mechanical support with left ventricular assist device bridge to transplantation. Recurrence of giant cell myocarditis was detected on surveillance endomyocardial biopsy 2 weeks after transplantation in a female patient without hemodynamic compromise. This was responsive to augmentation of immunosuppressive regimen. Antibody-mediated rejection occurred within the first month in a postpartum patient with elevated pre-transplant panel-reactive

antibody screen and this was treated with plasmapheresis. All patients had at least one episode of moderate cellular rejection within the first year of transplantation. Two patients developed early cardiac allograft vasculopathy and died after 3 and 5 years posttransplantation. A third patient died of metastatic lung carcinoma 8 years posttransplantation. The 1-year and 5-year survival rate in this cohort of patients was 100% and 80%, respectively.
Conclusions: In this single-center study, the rate of recurrence of GCM in the cardiac allograft is lower at 14% compared to previous reports. Our experience showed asymptomatic recurrence of GCM in one of 7 patients that resolved with increased immunosuppression. Overall posttransplantation survival in these patients are comparable to those with dilated cardiomyopathy and ischemic heart disease.

262 Isolated (Single Organ) Vasculitides, To Immunosuppress or Not To Immunosuppress

CD Tan, J Hernadez-Rodriguez, GS Hoffman, ER Rodriguez. Cleveland Clinic, Cleveland, OH.
Background: The pathology of vasculitides include a number of diseases that can affect large, medium and small vessels. In general they are thought to be systemic diseases and they are treated as such with systemic immunosuppression. Therapeutic decisions may be modulated by whether or not the vasculitis being treated is localized to an organ.
Design: Cases of possible isolated vasculitides of the breast or testes found in the databases of the Pathology and / or Rheumatology Departments of the Cleveland Clinic during the last 20 years were studied. Clinical information identified patients with local symptoms as opposed to systemic symptoms. Laboratory markers included erythrocyte sedimentation rate, C-reactive protein, blood count, and serologic tests. Review of the pathology included determination of the presence of absence of vasculitis, necrotizing vs. non necrotizing, type of inflammatory infiltrate, whether giant cells or granulomata were present.
Results: Four of 12 cases identified in the databases proved to have a diagnosis of vasculitis on surgical pathology examination of the tissue. Two were testicular vasculitis and 2 were breast vasculitis. The testicular vasculitis and one of the breast cases showed necrotizing vasculitis. The remaining breast case showed granulomatous vasculitis. Three of these four cases did not have systemic symptoms. The only one of with systemic symptoms was a case of necrotizing testicular vasculitis who also had fever for 1 month, chills, and myalgias and was treated with steroids for 5 months.
Conclusions: Single-organ involvement by vasculitis can be treated by excision only. Even necrotizing vasculitides can be a localized phenomenon that does not require systemic aggressive immunosuppression. The pathologic diagnosis of vasculitis needs to be correlated with clinical and laboratory information to formulate individualized treatment strategies. Clinico-pathologic correlation is imperative in these cases since it directly impacts treatment.

263 Rhythmic Wrinkling: A Pathologic Entity?

DA Troxclair, RR McGoey, WP Newman III. Louisiana State University Health Sciences Center, New Orleans, LA.
Background: Rhythmic wrinkling (RW) is the descriptive term assigned to observed areas of alternating intimal prominence that run perpendicular to the longitudinal axis of the aorta. This finding was first described in German literature in the early 20th century as Querlinien (cross lines) or Wellenlinien (wave lines). Recently, we published findings that support a role for RW in early, pre-clinical atherosclerosis. By examining aortas from 15-34 year old individuals collected in the Pathobiological Determinants of Atherosclerosis in Youth (PDAY) study, we demonstrated (1) aortic RW is relatively common and follows a specific distribution; and (2) RW occurs in the same topographical location as the more advanced, well-described, raised lesions (RL) of atherosclerosis. Consequently, we proposed that RW is a true pathologic entity, temporally related to early atherosclerosis. To date, we have not published histologic findings and, as such, have yet to define the cellular composition of rhythmic wrinkles.
Design: Longitudinal sections, taken perpendicular to the wrinkling, were processed and prepared for histologic analysis. Sections were stained with hematoxylin and eosin (H&E), Gomori van Gieson (GVG), oil-red-o (ORO) and smooth muscle actin (SMA).
Results: Histologic analysis supported the presence of RW as intimal areas of elevation and prominence bounded at their luminal margin by a single-layer of endothelial cells and at their deep margin by the internal elastic lamina (IEL). SMA stains were diffusely positive within the RW; while the elastin (GVG) and lipid (ORO) stains were negative.
Conclusions: These results begin to provide a microscopic – morphologic correlation for rhythmic wrinkling in the aorta. Preliminary histology suggests rhythmic wrinkles are intimal lesions composed primarily of smooth muscle cells. These findings add further support to the theory that RW is a true pathologic entity. And, with the previously published topographical results, we suggest that RW may represent an early morphologic manifestation of pre-clinical atherosclerosis. Additional studies are necessary and will focus on further characterizing RW, its microscopic composition, vascular location, periodicity and temporal relationship to raised lesions.

264 Expression of SmgGDS in Atherosclerotic Coronary Arteries

C Wynveen, D Firchau, L Gruman, CY Chen, HY Yang, R Thill, CL Williams, R Li. Medical College of Wisconsisn, Milwaukee, WI.
Background: Smooth muscle cells (SMCs), inflammatory cells, endothelial cells and platelets are all involved in the development of atherosclerosis. SMC proliferation and morphological alterations are known to have a role in this process. However, the underlying mechanism causing these changes is still unclear. Our preliminary in vitro studies revealed that SmgGDS, a guanine nucleotide exchange factor activating small GTPases, may enhance proliferation and induce morphological alterations of vascular SMCs. In order to correlate these in vitro findings with the development of atherosclerosis in humans, we used immunohistochemistry to observe the expression pattern of SmgGDS in human coronary arteries (CAs) of 41 autopsied patients with different levels of coronary artery atherosclerosis.
Design: Paraffin-embedded CAs from 41 consecutive autopsied adults (20 male and 21 female with an age range of 18-84; mean of 56.8) were divided into two groups based on the severity of atherosclerosis: 1) limited lesion (intimal thickening with up to 25% luminal occlusion); and 2) advanced lesion (>26% occlusion). Positive staining was defined as > 20% of smooth muscle cells with moderate or stronger staining intensity. Mononuclear inflammatory cells with moderate or stronger staining were also considered positive.
Results: SmgGDS was expressed in 18/41 (43.9%) of autopsied CAs. Of the 20 limited lesions, 14 (77.8%) were positive and 6 (26.1%) were negative. Of the 21 advanced lesions, only 4 (22.2%) were positive. The difference between the two groups was significant (P=0.001). In addition, 38/41 (92.7%) of the CAs showed plaque formation. Of these 38 cases, 26 (68.42%) showed SmgGDS expression in the mononuclear inflammatory cells within the plaques.
Conclusions: SmgGDS is frequently expressed in the smooth muscle of CAs with limited atherosclerosis and its expression is decreased in more advanced lesions. In addition, SmgGDS is also frequently expressed in inflammatory cells within the plaques. These findings suggest that SmgGDS may play a role in the development of atherosclerosis, especially at an early stage.

265 Has the 2004 Revision of the International Society of Heart and Lung Transplantation (ISHLT) Grading System Improved the Reproducibility of the Diagnosis and Grading of Cardiac Transplant Rejection?

H Yang, C Lai, T Baruch-Oren, S Ra, W Watts, WD Wallace, JA Kobashigawa, DW Gjertson, MC Fishbein. UCLA David Geffen School of Medicine, Los Angeles, CA.
Background: In 1990, the ISHLT created a working formulation to standardize the diagnosis and grading of cardiac transplant rejection. In 2004, the grading scheme was revised, such that prior grades 1A, 1B, and 2 were incorporated into a new grade 1R, prior grade 3A became grade 2R, and prior grade 3B and 4 became grade 3R. With better defined and fewer grades of cellular rejection, reproducibility was expected to improve.
Design: To test this hypothesis, we examined the interobserver reproducibility of both the 1990 and the 2004 Revised ISHLT Classification for Cardiac Allograft Rejection using Kappa statistics, generally regarded as the statistic of choice for measuring inter-observer agreement. Six independent observers (2 residents, 2 fellows, and 2 attending pathologists) graded the H&E stained slides of 175 endomyocardial biopsies according to the 1990 grading system. These grades were then converted into the 2004 revised grading system. The evaluation was carried out blindly and the agreement of the diagnoses was analyzed.
Results: The combined Kappa value of all grades diagnosed by all six reviewers was 0.369 for the 1990 grading system and 0.402 for the 2004 grading system (not statistically significant). Kappa values for grades 1B (0.265)/1R (0.397) and 3A(0.230)/2R(0.230) were lower than for all other grades, except grade 4 (0 = 0.466; 1A = 0.352; 2 = 0.508; 3B = 0.424; 4 = 0.239). Of note, combining the grades 3B and 4 (kappa values of 0.424 and 0.239, respectively) into one grade, 3R, did improve the agreement for high-grade lesions (grade 3R) (kappa value of 0.524).
Conclusions: In this study, the new 2004 ISHLT grading system for cardiac transplant rejection did not improve the inter-observer reproducibility when compared to the 1990 grading system, in large part because pathologists have difficulty in agreeing upon grades 1B/1R and 3A/2R rejection. In order to achieve better reproducibility with the current grading system, better criteria to define grades 1B/1R and 3A/2R are needed.

266 New Modes of Failure of Stentless Porcine Bioprostheses: An Analysis of 9 Explanted Freestyle ® Bioprosthesis

T Zhou, J Butany, SW Leong, KS Cunningham, A Jegatheeswaran. University Health Network, Toronto, ON, Canada.
Background: The Freestyle® valve is a porcine stentless valve, fixed in glutaraldehyde at physiological pressures and treated with alpha-amino oleic acid. It has excellent clinical and hemodynamic results; however, little is known about its long-term pathology or modes of failure.
Design: The 10 explanted valves were reviewed to assess the morphological changes and causes of bioprosthesis failure. This included gross and microscopic examination, and immunohistochemistry to identify the cellular response.
Results: One Freestyle® valve, explanted for mitral valve endocarditis on the fifth post-operative day, was excluded from analysis. Average implant duration was 52.8 ± 35.5 months (range 4 to 108 months). Four valves were explanted for infective endocarditis, three for aortic insufficiency and two for aortic stenosis. Cusp calcification was seen in five valves. Pannus and thrombus were seen in all valves. A chronic inflammatory reaction involving the xenograft arterial wall was seen in eight of nine valves, and was associated with significant damage to the porcine aortic tissue in seven cases, and porcine myocardial damage in six cases.
Conclusions: In our series : 1) Infective endocarditis was the cause of failure in 44% of cases (up to 50 months post implantation); 2) Pannus, thrombus and calcification, remain a concern; 3) A significant infiltrate of mononuclear cells (lymphocytes and macrophages) seen around the porcine aorta, was likely the cause of damage to the aortic media and its aneurysmal dilatation; 4) This inflammatory infiltrate and aortic wall damage is unusual and significant. In the cases wtih active infective endocarditis, it may be related to the infection. However, in the rest of the cases, it may in fact be a form of cellular rejection. **This finding has not been reported in any other bioprostheses and we believe is a new cause of bioprosthesis incompetence and failure.**